Long acting neurotensin synergizes with liraglutide to reverse obesity through a melanocortin-dependent pathway

Cecilia Ratner[1,2], Zhenyan He[3], Kaare V Grunddal[2], Louise J Skov[1,2], Bolette Hartmann[1,2], Fa Zhang[4], Annette Feuchtinger[5], Anette Bjerregaard[1,2], Christina Christoffersen[2,6], Matthias H Tschöp[7,8], Brian Finan[9], Richard D DiMarchi[4], Gina M Leinninger[10], Kevin W Williams[3], Christoffer Clemmensen[1], Birgitte Holst[1,2]

[1]NNF Center for Basic Metabolic Research, University of Copenhagen, Copenhagen, Denmark
[2]Department of Biomedical Sciences, University of Copenhagen, Copenhagen, Denmark
[3]Division of Hypothalamic Research, Department of Internal Medicine, University of Texas Southwestern Medical Center at Dallas, Dallas, TX, USA
[4]Department of Chemistry, Indiana University, Bloomington, IN, USA
[5]Research Unit Analytical Pathology, Helmholtz Zentrum München, Munich, Germany
[6]Department of Clinical Biochemistry, Rigshospitalet, Copenhagen, Denmark
[7]Institute for Diabetes and Obesity, Helmholtz Diabetes Center, Helmholtz Zentrum München, Munich, Germany
[8]Division of Metabolic Diseases, Department of Medicine, Technische Universität München, Munich, Germany
[9]Novo Nordisk Research Center Indianapolis, Indianapolis, IN, USA
[10]Department of Physiology, Michigan State University, East Lansing, MI, USA

Running title: Neurotensin and GLP-1 reverse obesity in synergy

Corresponding author:
Cecilia Ratner
NNF Center for Basic Metabolic Research and Department of Biomedical Sciences, University of Copenhagen, Copenhagen, Denmark
Phone: +45 22999320
Email: Cecilia.ratner@sund.ku.dk

Words: 4063

Figures: 7

Tables: 1

Diabetes Publish Ahead of Print, published online April 1, 2019

Abstract

Neurotensin, a gut hormone and neuropeptide, increases in circulation after bariatric surgery in rodents and humans and inhibits food intake in mice. However, its potential to treat obesity and the subsequent metabolic dysfunctions have been difficult to assess owing to its short half-life *in vivo*. Here, we demonstrate that a long acting, pegylated analogue of the neurotensin peptide (P-NT) reduces food intake, body weight and adiposity in diet-induced obese (DIO) mice when administered once daily for 6 days. Strikingly, when P-NT was combined with the GLP-1 mimetic liraglutide the two peptides synergized to reduce food intake and body weight relative to each mono-therapy, without inducing a taste aversion. Further, P-NT and liraglutide co-administration improved glycemia and reduced steatohepatitis. Finally, we show that the melanocortin pathway is central for P-NT-induced anorexia and necessary for the full synergistic effect of P-NT and liraglutide combination-therapy. Overall, our data suggest that P-NT and liraglutide combination-therapy could be an enhanced treatment for obesity with improved tolerability compared to liraglutide mono-therapy.

The prevalence of obesity and diabetes has reached epidemic proportions and is still on the rise (1). Despite this, a limited number of anti-obesity drugs are currently approved, including the glucagon-like peptide-1 (GLP-1) analogue liraglutide. However, liraglutide and other obesity pharmacotherapies evoke only modest weight loss of 5-10% (2). To improve efficacy and limit unacceptable adverse effects, a current innovation in the development of anti-obesity treatments involves targeting multiple signaling pathways simultaneously. This approach has several advantages including exploiting additive or synergistic effects between distinct signaling pathways, and is supported by the marked weight loss associated with bariatric surgery, which broadly stimulates anorexigenic hormone release (3). Further, tolerability is expected to improve with combination-treatments as lower doses of each agent could be used. With mono-therapy, adverse effects are often reported due to the usage of peak doses. For example, upwards of 30-40% of patients on therapeutic doses of liraglutide suffer from nausea in a dose-dependent manner (4; 5).

Combinatorial treatment approaches have thus far largely been explored for GLP-1 mimetics (6) in combination with a range of other hormones including leptin (7), peptide YY (PYY) (8), cholecystokinin (9), amylin (10) and glucagon/glucose-dependent insulinotropic polypeptide (11) either as adjunctive co-treatments or as co-agonist fusion peptides. We recently demonstrated that, in addition to the expression in N-cells, the gut hormone neurotensin (NT) is co-expressed with GLP-1 and PYY in L-cells (12), suggesting a common functional importance.

NT is generally considered an anorexigenic neuropeptide and reduces food intake when administered directly into the brain (13-15). Further, NT is increased in circulation following gastric bypass surgery in rodents and humans (16-18), which we demonstrated might contribute to the subsequent hypophagia (16). The metabolic

effects of peripheral NT are, however, incompletely understood, which may relate to the challenges working with peptide hormones with short circulatory half-lives such as NT, where the half-life is estimated to 30 s in rodents (19). To improve the understanding of NT effects on metabolism, we have developed a long-acting NT peptide (pegylated NT, P-NT)(16). P-NT prolongs the inhibition of feeding in mice at least ten times compared to native NT (16) but its effects in a chronic setting as well as its downstream targets are incompletely understood. We hypothesized that long-acting NT and GLP-1 mimetics converge in the central melanocortin pathway but through different intracellular signaling pathways, $G\alpha_q$ and $G\alpha_s$ respectively, to reduce food intake and reverse obesity.

Research design and methods

Animals

Male C57Bl/6J mice (Janvier, Le Genest-Saint-Isle, France) were used as wildtype lean or diet-induced obese (DIO) mice. DIO mice were fed a high-fat high-sucrose diet (58% fat; #D12331, Research diets, New Brunswick, NJ) from 7 weeks of age for 4-6 months. Lean mice were fed a chow diet (altromin 1310, Lage, Germany). Mice were housed in temperature-controlled environments under a 12/12 h light-dark cycle with ad libitum access to food and water unless otherwise stated. Animal experiments using wildtype lean or DIO mice and male loxTB melanocortin 4 receptor (MC4R) mice (20) (B6;129S4-*Mc4r*^{tm1Lowl}/J stock no: 006414; Jackson Laboratory, Bar Harbor, ME) were approved by the Danish animal inspectorate or the Animal Use and Care Committee of Bavaria, Germany and followed institutional guidelines. Electrophysiology studies using Pomc-hrGFP mice (21) were performed in

accordance with the guidelines established by the National Institute of Health Guide for the Care and Use of Laboratory Animals and approved by the University of Texas Institutional Animal Care and Use Committee.

Peptides

The side-chain protected NT with a KKGG linker at N-terminal was assembled by automated synthesis employing an ABI-433A peptide synthesizer with standard Fmoc/6-Cl-HOBt/DIC coupling protocols. The crude peptide was acylated with 20K PEG NHS ester (Iris Biotech GmbH, Marktredwitz, Germany). The desired PEG-peptide was purified by preparative reverse-phase HPLC, final peptide-deprotection was conducted and a second preparative HPLC purification was performed. MALDI analysis confirmed the molecular weight of the final product.

Liraglutide was provided by Novo Nordisk (Indianapolis, IN or Måløv, Denmark). All peptides were solubilized in saline. Liraglutide was dosed in a concentration of 2, 3 or 8 nmol/kg equivalent of 7.5, 11.3 and 30 μg/kg respectively as indicated in figure legends. Importantly, to allow a sufficient window for weight loss synergy subthreshold doses of liraglutide were used and each batch of liraglutide was independently dose-optimized. P-NT was dose-optimized in concentrations ranging from 44-1188 nmol/kg in 3-fold increments in DIO mice both as a mono-treatment and in combination with liraglutide. A dose of 396 nmol/kg P-NT was used in additional experiments. P-NT and liraglutide co-treatment was administered by single formulated injections. Peptides were dosed at a volume of 5 mL/kg subcutaneously.

Food intake, body weight and indirect calorimetry

DIO and MC4R KO mice (n=5-8 as indicated in figure legends) were single-housed or housed in pairs and treated daily for 2-6 days as indicated in figures with vehicle, liraglutide, P-NT, or co-treatment with liraglutide and P-NT in the end of the light phase. One cohort of DIO mice (n=8) was placed in an indirect calorimetry system (TSE systems, Bad Homburg, Germany) during peptide treatment where food intake, respiratory exchange ratio (RER), energy expenditure and activity levels were continuously monitored for 72 hours. Body composition was assessed using MRI (EchoMRI, Houston, TX). MC4R KO mice were fed a high-fat high-sucrose diet (D12331, Research diets) for 5 weeks prior to pharmacological treatment. Weight-matched DIO C57Bl/6J mice served as controls for MC4R KO mice. After a 1-week washout period, the effect of a 10x dose of liraglutide (20 nmol/kg; 75 μg/kg) was assessed in MC4R KO and weight-matched DIO controls.

Tissue collection for blood biochemistry, liver histology and qPCR

Tissue was collected after 6 days of treatment in DIO mice. On the day of sacrifice, mice were fasted for 4 h, blood sampling was done from the tail vein and glucose measured using a glucometer before mice received an injection of peptides before sacrifice and tissue collection 2 h later. Liver samples were immersed in 4% paraformaldehyde or snap frozen in liquid nitrogen and plasma was collected in EDTA-coated tubes, centrifuged at 3000 *g,* 15 min, 4°C and stored at -80°C.

Blood biochemistry

Lipoprotein separation was performed using size exclusion chromatography with 120 μL pooled plasma from the treatment groups as previously described (22). The following kits were used for remaining analyses: Cholesterol (Thermo Scientific,

Waltham, MA), triglycerides (Wako Chemicals, Neuss, Germany), insulin (mesoscale Discoveries, Rockville, MD) and leptin (mesoscale Discoveries).

Liver histology

Excised liver samples were fixed in 4% formalin, embedded in paraffin and cut into 3 μm slices for hematoxylin and eosin (H&E) staining. The H&E slides were evaluated using a brightfield microscope (Axioplan, Zeiss, Oberkochen, Germany). The steatohepatitis score was defined as the unweighted sum of the individual score for steatosis and lobular inflammation. Steatosis and lobular inflammation was scored as previously described (23). Total scores ranged from 0 to 6 with score 0 considered no steatohepatitis, scores 1 and 2 considered borderline steatohepatitis, scores 3 and 4 considered onset steatohepatitis and score 5 and 6 considered definite steatohepatitis.

Quantitative polymerase chain reaction

Liver RNA was extracted using the RNeasy lipid tissue mini kit (Qiagen, Hilden, Germany) with DNAse digestion according to the manufacturer's instructions. cDNA was synthesized from RNA matched samples using the superscript III Reverse Transcriptase kit (Thermo Fisher Scientific, Waltham, MA). qPCR was performed using PrecisionPLUS Mastermix on a LightCycler480 (Roche Applied Science, Penzberg, Germany). Relative gene expression was calculated using the $\Delta\Delta C_t$ method normalizing to the average value of the reference genes TATA-box binding protein (*TBP*) and hypoxanthine-guanine phosphoribosyltransferase (*HPRT*). See table S1 for primers.

Taste aversion

Taste aversion was performed in lean mice (n=8) as previously described (16). During conditioning, mice received injections of vehicle, liraglutide (3 nmol/kg), P-NT (396 nmol/kg), combination-treatment with liraglutide (3 nmol/kg) and P-NT (396 nmol/kg) or LiCl (3 mmol/kg), which served as a positive control.

Pharmacokinetic profiling

Lean mice (n=4) were treated with vehicle, P-NT (396 nmol/kg), liraglutide (3 nmol/kg) or co-treatment with liraglutide (3 nmol/kg) and P-NT (396 nmol/kg). Blood was drawn from the tail vein at the indicated time-points into EDTA-coated tubes, centrifuged at 3000 *g,* 15 min, 4°C and stored at -80°C. Intact NT was measured as previously described (24).

Oral glucose tolerance test

DIO mice (n=14) were treated with a single dose of vehicle, liraglutide (2 nmol/kg), P-NT (396 nmol/kg) or combination-treatment 1 hour prior to glucose administration (1 g/kg p.o.) to assess the acute effect of the peptides on glucose tolerance. Blood glucose was measured from the tail vein using a glucometer and insulin was measured in retro-orbital vein samples at the indicated time points.

Taste preference

Taste preference during peptide treatment was evaluated between regular chow and a palatable medium-fat high-sucrose diet (Condensed milk diet, D12266B, Research diets). Single-housed DIO mice were provided with both diets in separate compartments in the wire cage top equidistant from the water bottle. Fresh diet was provided daily. Baseline preference was assessed during 6 days. After this, mice were

divided into treatment groups with comparable baseline diet preference and body weight and diet preference was assessed in 2 separate experiments. First, mice had 2 days access to either chow or condensed milk diet followed by 2 days access to the same diet during treatment with vehicle, P-NT (396 nmol/kg), liraglutide (2 nmol/kg) or combination treatment. After a 1-week washout period the mice were switched to the opposite diet and the protocol was repeated and the ability of the treatments to inhibit the intake of the 2 diets was compared. Another cohort of DIO mice had access to both diets simultaneously during peptide injections and the data is presented as intake of condensed milk diet/total intake.

Electrophysiology

Pomc-hrGFP mice (21) were used to identify Pomc neurons in the arcuate nucleus of the hypothalamus. Brain slices were prepared from male mice (5–8 weeks old) and electrophysiology performed as previously described (25-27). NT (100 nM; Polypeptide, Hillerød, Denmark), liraglutide (100 nM) and tetrodotoxin (TTX; 2 μM; Tocris; Bristol, UK) were added to the artificial cerebrospinal fluid for specific experiments. Solutions containing drug were typically perfused for 5 min. A drug effect was required to be associated temporally with peptide application, and the response had to be stable within a few min. A neuron was considered depolarized if a change in membrane potential was at least 2 mV in amplitude. *n* represents the number of cells studied.

Multiplex fluorescence in situ hybridization

Brains from lean wildtype mice were frozen in powdered dry ice and sectioned on a cryostat into 12 μm thick coronal sections that were collected from the arcuate

nucleus. *In situ* hybridization was performed according to manufacturers instructions using the RNAscope® Multiplex Fluorescent Reagent Kit v2 (Advanced Cell Diagnostics (ACD), Newark, CA) and PerkinElmer TSA® Plus fluorescein, Cyanine 3 and Cyanine 5 Systems (PerkinElmer, Waltham, MA). Probes targeting mm-Pomc (Cat.No. 314081-C3, ACD), mm-NtsR1 (Cat.No. 422411, ACD), mm-GLP-1R (Cat.No. 418851-C2, ACD), mm-Ppib (Cat.No. 313911, ACD) and DapB (Cat.No. 310043, ACD) were used. Images were captured using a laser scanning confocal microscope (LSM700, Zeiss).

Statistics

Data was tested for statistical significance using Graphpad Prism except for ANCOVA, which was performed using SAS. T-test, Mann-Whitney non-parametric test, two-way ANOVA repeated measurements, two-way ANOVA and one-way ANOVA were performed with appropriate multiple comparison's test as indicated in figure legends. Energy expenditure data was analyzed using ANCOVA with body weight as covariate. All data are represented as mean ± SD. The level of significance was set at $p<0.05$.

Results

Combination-treatment with P-NT and liraglutide reduces body weight and food intake in DIO mice

Optimization of the P-NT dose showed that increasing the dose from 396 nmol/kg to 1188 nmol/kg both as a mono-therapy and in combination with liraglutide did not result in improved weight loss or food intake inhibition (Fig. S1A-B). Decreasing the

P-NT dose below 396 nmol/kg to 132 nmol/kg and 44 nmol/kg negatively impacted the ability of P-NT to reduce food intake and body weight as a mono-therapy, however, in combination with liraglutide, the 132 nmol/kg dose showed equal efficiency as the 396 nmol/kg dose (Fig. S1C-D). For remaining experiments, the 396 nmol/kg dose was used.

During 6 days of daily treatment, P-NT mono-therapy reduced food intake and body weight while liraglutide was not significantly different from vehicle-treated mice. Mice co-treated with P-NT and liraglutide lost approximately 8% (4 g) of their body weight and a synergistic effect of the peptides was observed on feeding inhibition and body weight loss (Fig. 1A-B). The weight loss was predominantly due to loss of fat mass (Fig. 1C-D). Mice in the combination-treatment group had decreased insulin and leptin levels compared to vehicle reflecting the weight loss in this group (Table 1). Mice treated with P-NT and liraglutide combination-treatment also had lower glucose levels, and this appeared to be driven by liraglutide (Table 1).

Combination-treatment with P-NT and liraglutide does not affect energy expenditure or induce a taste aversion

To further understand the mechanism for the observed weight loss indirect calorimetry was performed. No differences were observed between groups in energy expenditure and activity levels (Fig. 2A-C), while a reduction in the RER value was found after combination-treatment reflecting increased lipid oxidation (Fig. 2D). Food intake and body weight were reduced in a synergistic manner following P-NT and liraglutide combination-treatment relative to mono-therapies (Fig. 2E-F). Vehicle-treated mice that were pair-fed to the combination-treatment had a weight loss similar to that of the combination treatment group, suggesting that energy expenditure did not

contribute to the phenotype (Fig. 2G). To establish if the decreased food intake could be due to nausea as previously described for peak doses of liraglutide (28-30) a taste aversion experiment was performed. P-NT, subthreshold liraglutide dose, or the combination of P-NT and liraglutide did not cause a conditioned taste aversion, whereas injections of the positive control LiCl induced an aversion towards saccharin (Fig. 2H).

The exposure time in plasma of P-NT was similar when administered alone or in combination with liraglutide and plasma NT levels were elevated above baseline for up to 48 h (Fig. 2I). In comparison, native NT is cleared in just 15 min using the same method (16). Finally, we assessed if P-NT and liraglutide mono-and combination-treatment affected taste preference. When mice were given the choice between chow and a palatable medium-fat high-sucrose diet (condensed milk diet), we found no changes in their diet preference following peptide treatment (Fig. 2J). Further, we found no differences in the ability of P-NT and liraglutide mono-and combination-treatment to inhibit the intake of chow versus the condensed milk diet, indicating that the treatments did not affect taste preference (Fig. 2 K-L).

The melanocortin system is central for P-NT and P-NT and liraglutide combination-treatment efficacy

In accordance with previous publications (31; 32), we found that NtsR1 and GLP-1R were expressed in Pomc neurons in the arcuate nucleus and that numerous Pomc neurons co-expressed both NtsR1 and GLP-1R using *in situ* hybridization (Fig. 3A-B; positive and negative controls fig. S2). Next, we assessed if NT increases the firing rate of arcuate Pomc neurons in Pomc-eGFP mice. NT (100 nM) depolarized Pomc neurons (change of resting membrane potential: +5.5 ± 0.5 mV, n=7; Fig. 4A-E,G).

Similar to previous reports studying GLP1(31), we found that liraglutide (100 nM) depolarized Pomc neurons to a similar degree (change of resting membrane potential: +6.4 ± 0.3 mV, n=3; Figure 4G). Notably, combined administration with NT (100 nM) and liraglutide (100 nM) resulted in a larger depolarization of Pomc neurons (change of resting membrane potential: +10.9 ± 0.7 mV; n = 5; Fig. 4F-G). These data suggest that liraglutide can enhance the NT-induced excitatory effect on Pomc neurons. The depolarization induced by NT and combination treatment with NT and liraglutide was observed in the presence of TTX (2 μM; +7.4 ± 0.2 mV (NT), n=4 and +11.5 ± 2.0 mV (NT+liraglutide); n = 5, Fig. S3A-C), indicative of a direct membrane depolarization independent of action potential-mediated synaptic transmission.

Finally, we tested the effect of P-NT and liraglutide mono-and combination-therapy in MC4R KO mice compared to weight-matched DIO controls during 3 days of treatment. MC4R KO mice were unresponsive to the anorexigenic and body weight reducing effect of P-NT (Fig. 5B and E). MC4R KO and DIO control mice showed no response to sub-threshold liraglutide mono-therapy (Fig. 5A and D), however, a 10x dose of liraglutide evoked a larger anorexic and body weight reducing response in DIO control mice compared to MC4R KO mice (Fig. S4A-B). MC4R KO mice decreased their food intake and body weight after P-NT and liraglutide combination-therapy but their response was blunted compared to DIO controls (Fig. 5C and F). Loss of fat and lean mass was likewise blunted in MC4R KO mice compared to DIO controls following P-NT mono-therapy and P-NT and liraglutide combination-therapy (Fig. 5G-H), overall suggesting that the melanocortin pathway is important for P-NT induced appetite regulation and body weight reduction.

Acute P-NT and liraglutide combination-treatment does not affect glucose tolerance

We evaluated the acute effect of P-NT and liraglutide treatment on glucose homeostasis using an oral glucose tolerance test in DIO mice. P-NT lowered the glucose level at the 15-minute time-point compared to vehicle and liraglutide mono-therapy (Fig. 6A). However, overall no differences in glucose levels (area under the curve) were observed between groups (Fig. 6B), as P-NT slightly delayed the glucose excursion. Insulin levels were likewise similar after acute peptide treatment (Fig. 6C).

P-NT and liraglutide combination-treatment reduces steatohepatitis

We observed a modest improvement in steatohepatitis in the P-NT and the P-NT and liraglutide combination-treatment group in DIO mice after 6 days of treatment (Fig. 7A-B). This was accompanied by a reduction in *PCSK9* expression in the combination-treatment group suggestive of increased removal of cholesterol from circulation, while major hepatic bile acid metabolism pathways were not regulated (Fig. 7C-D). Although total plasma cholesterol was not statistically different between groups (Fig. 7E), LDL-cholesterol was substantially reduced in the combination treatment group, while HDL-cholesterol showed a more modest decrease (Fig. 7F).

Discussion

The lack of safe and effective pharmacotherapies to treat obesity and associated disorders combined with a growing burden of metabolic diseases worldwide, highlight the need for new treatment strategies. A pioneering approach to improve pharmacological efficacy has focused on combination-therapies to obtain superior efficacy and better tolerability compared to mono-therapies. In the present study, we find that a pegylated version of the gut hormone NT reduced food intake, body weight

and adiposity in DIO mice. Intriguingly, when P-NT was combined with a sub-threshold dose of the GLP-1 mimetic liraglutide, the two peptides exerted a synergistic reduction in body weight and food intake in obese mice relative to each mono-therapy. Our indirect calorimetry and pair-feeding data suggest that altered activity and energy expenditure were not contributing to the weight phenotype. Further, glucose homeostasis and liver function were improved following chronic liraglutide and combination-treatment respectively demonstrating an overall improvement in metabolic disorders. Finally, we found that the melanocortin pathway is central for the anorexigenic effect of P-NT and the synergy observed between liraglutide and P-NT.

Currently, liraglutide mono-therapy constitutes one of the safest treatment options for obesity but only elicits modest weight loss in humans (2) and problems with compliance exists mainly due to nausea, which is experienced for upwards of 30-40% of patients (4; 5). This is likewise seen in rodents where peak doses of liraglutide induce a taste aversion towards associated flavors (28-30). Thus, it is desirable to improve tolerability by employing lower liraglutide doses while maintaining efficacy by combining it with another weight reducing agent that does not evoke nausea and emesis. In the present study, we demonstrate this principle by combining liraglutide with P-NT. Sub-threshold dosing of the mono-therapies give rise to modest improvements in body weight but, when administered in combination, liraglutide and P-NT synergize to amplify anorexigenic signaling without inducing taste aversion. NT has previously been described to have varying effects on glucose homeostasis (33). Here we found that acute treatment with P-NT and sub-threshold liraglutide mono-and combination-therapy did not result in improvements in glucose control or insulin levels. However, following 6-days treatment, glucose and insulin levels

significantly improved in mice that were treated with liraglutide and the combination of P-NT and liraglutide, suggesting that liraglutide drives the chronic benefits on glucose metabolism.

We also observed modest improvements in steatohepatitis, decreased plasma LDL-cholesterol and changes in liver gene expression suggestive of improved hepatic lipid handling and removal of cholesterol from the blood following 6 days of combination-treatment in DIO mice. Recent clinical studies report discrepant results regarding the association between circulating NT levels and non-alcoholic fatty liver disease (34; 35). Although previous studies report the presence of NtsR1 in the liver in some species (36; 37), we did not find any NtsR1 expression in mouse liver using qPCR (data now shown). The lack of NtsR1 expression in liver is supported by results in human and mouse databases (www.proteinatlas.org, www.informatics.jax.org/assay/MGI:3625053). Therefore, the reduced steatohepatitis in our study is most likely an indirect mechanism potentially contributable to the weight loss of the mice.

The downstream mechanism by which peripheral NT reduces food intake is largely unexplored. We previously showed that NT-induced anorexia persists in vagotomized mice pointing to a direct effect in the brain of NT (16). The NtsR1 is widely expressed centrally with high levels in both homeostatic i.e. hypothalamus and hedonic i.e. the ventral tegmental area food intake regulating regions (38). Due to the size and hydrophilic nature of the PEG modification of our NT peptide, the effects seen in the present study are more likely to be mediated via brain areas with a compromised blood-brain-barrier such as the arcuate nucleus of the hypothalamus. This is supported by our taste preference data, showing that P-NT and liraglutide mono-and combination-treatment exert the same level of inhibition on diets of

varying palatability pointing to homeostatic feeding regulation. In the arcuate nucleus, the NtsR1 is present on both Pomc and AgRP neurons (32). Following acute P-NT treatment we previously observed an upregulation of Pomc expression in the arcuate nucleus while AgRP and NPY were not regulated (16). Thus, here we focused on Pomc neurons in our characterization of the downstream effectors of P-NT and liraglutide therapy. We found that Pomc neurons co-expressed the NtsR1 and the GLP-1R. Further, Pomc neurons were depolarized in response to NT and the change in membrane potential was augmented with liraglutide co-application. These effects persisted in the presence of TTX indicative of a direct effect on Pomc neurons independent of synaptic transmission. Next, we assessed the effect of P-NT and liraglutide mono-and combination-therapy in MC4R KO mice in comparison to weight-matched DIO control mice. MC4R KO mice were unresponsive to the anorexic and body weight lowering effects of P-NT mono-therapy and showed a blunted response to P-NT and liraglutide combination- therapy. This suggests that the melanocortin pathway is essential for P-NT-induced anorexia and necessary for P-NT and liraglutide to synergize in their regulation of food intake and body weight. Liraglutide reduces food intake when micro-injected into the arcuate nucleus (39) and Pomc neurons have been suggested as important downstream effectors of liraglutide-induced anorexia (31). However, others have challenged the necessity of Pomc neurons for liraglutide to reduce food intake (30; 40; 41) and a model where several sites and neuronal populations in the brain contribute to liraglutide-induced anorexia is emerging (42). As the anorexigenic and body weight lowering effects of medium dose liraglutide mono-therapy (20 nmol/kg) were blunted in MC4R KO mice compared to DIO controls in our study, our data suggest that liraglutide can partly act through this pathway. We therefore hypothesize that NT and liraglutide converge on

the same population of Pomc neurons to reverse obesity but through different intra-cellular signaling pathways as NT is $G\alpha_q$-coupled while GLP-1 acts through $G\alpha_s$. The $G\alpha_q$ and $G\alpha_s$ signaling pathways have previously been described to synergize in other cellular systems (43). Future studies should map out the exact contribution of the different intracellular signaling events underlying the observed synergy between P-NT and liraglutide.

In conclusion, we developed a stable long-acting analogue of NT enabling us to establish the impact of sustained NT signaling on metabolic homeostasis. We demonstrate a synergistic action between GLP-1 and NT mediated pathways in the regulation of food intake and body weight, and show that P-NT in combination with sub-threshold doses of liraglutide reverse obesity and metabolic syndrome without the concurrent induction of nausea seen with peak dose liraglutide mono-therapy. Finally, we identify the melanocortin pathway as a key downstream effector circuit for P-NT action in the brain and suggest that P-NT and liraglutide may synergize in Pomc neurons via segregated intra-cellular signaling pathways.

Acknowledgements and funding

We thank Dr. Joel K. Elmquist (of the Division of Hypothalamic Research, Department of Internal Medicine, UT Southwestern Medical Center, Dallas, Texas) for kindly providing us with the Pomc-hrGFP mice. We thank Lisbeth Meyer Petersen for technical assistance. We acknowledge the Core Facility for Integrated Microscopy, Faculty of health and Medical Sciences, University of Copenhagen. This work was funded by the Novo Nordisk Foundation and The A.P. Møller Foundation. CR was supported by a Postdoctoral grant from the Lundbeck Foundation and KWW

was supported by grants from the US National Institutes of Health (Grant R01-DK100699 and DK119169).

Author contributions: CR co-conceptualized, researched and interpreted data and wrote the manuscript, KVG, LJS, CC (Christina Christoffersen), AB and BH (Bolette Hartmann) researched and interpreted data and reviewed the manuscript, ZH and KWW performed electrophysiology studies and interpreted data, FZ and MHT provided resources, RDD, BF and GML provided resources and reviewed the manuscript, AF performed liver histology, CC (Christoffer Clemmensen) co-conceptualized, researched and interpreted data and reviewed the manuscript and BH (Birgitte Holst) co-conceptualized, interpreted data and reviewed the manuscript. All authors approved the manuscript. CR is the guarantor of the manuscript and takes responsibility for the content of the publication. BF and RDD are employees of Novo Nordisk and MHT serves as a SAB member of ERX Pharmaceuticals, Inc., Cambridge, MA. The Institute for Diabetes and Obesity receives research support from Novo Nordisk and Sanofi-Aventis. The remaining authors declare no conflict of interest. Parts of this work have previously been presented at the Neurobiology of Obesity Symposium, Aberdeen, Scotland, August 2017.

References

1. Wang YC, McPherson K, Marsh T, Gortmaker SL, Brown M: Health and economic burden of the projected obesity trends in the USA and the UK. Lancet 2011;378:815-825
2. Heymsfield SB, Wadden TA: Mechanisms, Pathophysiology, and Management of Obesity. N Engl J Med 2017;376:254-266
3. Stefanidis A, Oldfield BJ: Neuroendocrine mechanisms underlying bariatric surgery: Insights from human studies and animal models. J Neuroendocrinol 2017;29
4. Marino AB, Cole SW, Nuzum DS: Alternative dosing strategies for liraglutide in patients with type 2 diabetes mellitus. Am J Health Syst Pharm 2014;71:223-226
5. Bettge K, Kahle M, Abd El Aziz MS, Meier JJ, Nauck MA: Occurrence of nausea, vomiting and diarrhoea reported as adverse events in clinical trials studying glucagon-like peptide-1 receptor agonists: A systematic analysis of published clinical trials. Diabetes Obes Metab 2017;19:336-347
6. Finan B, Clemmensen C, Muller TD: Emerging opportunities for the treatment of metabolic diseases: Glucagon-like peptide-1 based multi-agonists. Mol Cell Endocrinol 2015;418 Pt 1:42-54
7. Muller TD, Sullivan LM, Habegger K, Yi CX, Kabra D, Grant E, Ottaway N, Krishna R, Holland J, Hembree J, Perez-Tilve D, Pfluger PT, DeGuzman MJ, Siladi ME, Kraynov VS, Axelrod DW, DiMarchi R, Pinkstaff JK, Tschop MH: Restoration of leptin responsiveness in diet-induced obese mice using an optimized leptin analog in combination with exendin-4 or FGF21. J Pept Sci 2012;18:383-393
8. Neary NM, Small CJ, Druce MR, Park AJ, Ellis SM, Semjonous NM, Dakin CL, Filipsson K, Wang F, Kent AS, Frost GS, Ghatei MA, Bloom SR: Peptide YY3-36 and glucagon-like peptide-17-36 inhibit food intake additively. Endocrinology 2005;146:5120-5127
9. Trevaskis JL, Sun C, Athanacio J, D'Souza L, Samant M, Tatarkiewicz K, Griffin PS, Wittmer C, Wang Y, Teng CH, Forood B, Parkes DG, Roth JD: Synergistic metabolic benefits of an exenatide analogue and cholecystokinin in diet-induced obese and leptin-deficient rodents. Diabetes Obes Metab 2015;17:61-73
10. Trevaskis JL, Mack CM, Sun C, Soares CJ, D'Souza LJ, Levy OE, Lewis DY, Jodka CM, Tatarkiewicz K, Gedulin B, Gupta S, Wittmer C, Hanley M, Forood B, Parkes DG, Ghosh SS: Improved glucose control and reduced body weight in rodents with dual mechanism of action peptide hybrids. PLoS One 2013;8:e78154
11. Finan B, Yang B, Ottaway N, Smiley DL, Ma T, Clemmensen C, Chabenne J, Zhang L, Habegger KM, Fischer K, Campbell JE, Sandoval D, Seeley RJ, Bleicher K, Uhles S, Riboulet W, Funk J, Hertel C, Belli S, Sebokova E, Conde-Knape K, Konkar A, Drucker DJ, Gelfanov V, Pfluger PT, Muller TD, Perez-Tilve D, DiMarchi RD, Tschop MH: A rationally designed monomeric peptide triagonist corrects obesity and diabetes in rodents. Nat Med 2015;21:27-36
12. Grunddal KV, Ratner CF, Svendsen B, Sommer F, Engelstoft MS, Madsen AN, Pedersen J, Nohr MK, Egerod KL, Nawrocki AR, Kowalski T, Howard AD, Poulsen SS, Offermanns S, Backhed F, Holst JJ, Holst B, Schwartz TW: Neurotensin Is Coexpressed, Coreleased, and Acts Together With GLP-1 and PYY in Enteroendocrine Control of Metabolism. Endocrinology 2016;157:176-194

13. Cooke JH, Patterson M, Patel SR, Smith KL, Ghatei MA, Bloom SR, Murphy KG: Peripheral and central administration of xenin and neurotensin suppress food intake in rodents. Obesity (Silver Spring) 2009;17:1135-1143
14. de Beaurepaire R, Suaudeau C: Anorectic effect of calcitonin, neurotensin and bombesin infused in the area of the rostral part of the nucleus of the tractus solitarius in the rat. Peptides 1988;9:729-733
15. Hawkins MF, Barkemeyer CA, Tulley RT: Synergistic effects of dopamine agonists and centrally administered neurotensin on feeding. Pharmacol Biochem Behav 1986;24:1195-1201
16. Ratner C, Skov LJ, Raida Z, Bachler T, Bellmann-Sickert K, Le Foll C, Sivertsen B, Dalboge LS, Hartmann B, Beck-Sickinger AG, Madsen AN, Jelsing J, Holst JJ, Lutz TA, Andrews ZB, Holst B: Effects of Peripheral Neurotensin on Appetite Regulation and Its Role in Gastric Bypass Surgery. Endocrinology 2016;157:3482-3492
17. Dirksen C, Jorgensen NB, Bojsen-Moller KN, Kielgast U, Jacobsen SH, Clausen TR, Worm D, Hartmann B, Rehfeld JF, Damgaard M, Madsen JL, Madsbad S, Holst JJ, Hansen DL: Gut hormones, early dumping and resting energy expenditure in patients with good and poor weight loss response after Roux-en-Y gastric bypass. Int J Obes (Lond) 2013;37:1452-1459
18. Naslund E, Gryback P, Hellstrom PM, Jacobsson H, Holst JJ, Theodorsson E, Backman L: Gastrointestinal hormones and gastric emptying 20 years after jejunoileal bypass for massive obesity. Int J Obes Relat Metab Disord 1997;21:387-392
19. Aronin N, Carraway RE, Ferris CF, Hammer RA, Leeman SE: The stability and metabolism of intravenously administered neurotensin in the rat. Peptides 1982;3:637-642
20. Balthasar N, Dalgaard LT, Lee CE, Yu J, Funahashi H, Williams T, Ferreira M, Tang V, McGovern RA, Kenny CD, Christiansen LM, Edelstein E, Choi B, Boss O, Aschkenasi C, Zhang CY, Mountjoy K, Kishi T, Elmquist JK, Lowell BB: Divergence of melanocortin pathways in the control of food intake and energy expenditure. Cell 2005;123:493-505
21. Parton LE, Ye CP, Coppari R, Enriori PJ, Choi B, Zhang CY, Xu C, Vianna CR, Balthasar N, Lee CE, Elmquist JK, Cowley MA, Lowell BB: Glucose sensing by POMC neurons regulates glucose homeostasis and is impaired in obesity. Nature 2007;449:228-232
22. Christoffersen C, Jauhiainen M, Moser M, Porse B, Ehnholm C, Boesl M, Dahlback B, Nielsen LB: Effect of apolipoprotein M on high density lipoprotein metabolism and atherosclerosis in low density lipoprotein receptor knock-out mice. J Biol Chem 2008;283:1839-1847
23. Jall S, Sachs S, Clemmensen C, Finan B, Neff F, DiMarchi RD, Tschop MH, Muller TD, Hofmann SM: Monomeric GLP-1/GIP/glucagon triagonism corrects obesity, hepatosteatosis, and dyslipidemia in female mice. Mol Metab 2017;6:440-446
24. Kuhre RE, Bechmann LE, Wewer Albrechtsen NJ, Hartmann B, Holst JJ: Glucose stimulates neurotensin secretion from the rat small intestine by mechanisms involving SGLT1 and GLUT2, leading to cell depolarization and calcium influx. Am J Physiol Endocrinol Metab 2015;308:E1123-1130
25. Sun J, Gao Y, Yao T, Huang Y, He Z, Kong X, Yu KJ, Wang RT, Guo H, Yan J, Chang Y, Chen H, Scherer PE, Liu T, Williams KW: Adiponectin potentiates the acute effects of leptin in arcuate Pomc neurons. Mol Metab 2016;5:882-891

26. Yao T, Deng Z, Gao Y, Sun J, Kong X, Huang Y, He Z, Xu Y, Chang Y, Yu KJ, Findley BG, Berglund ED, Wang RT, Guo H, Chen H, Li X, Kaufman RJ, Yan J, Liu T, Williams KW: Ire1alpha in Pomc Neurons is Required for Thermogenesis and Glycemia. Diabetes 2016;
27. Gao Y, Yao T, Deng Z, Sohn JW, Sun J, Huang Y, Kong X, Yu KJ, Wang RT, Chen H, Guo H, Yan J, Cunningham KA, Chang Y, Liu T, Williams KW: TrpC5 Mediates Acute Leptin and Serotonin Effects via Pomc Neurons. Cell Rep 2017;18:583-592
28. Sisley S, Gutierrez-Aguilar R, Scott M, D'Alessio DA, Sandoval DA, Seeley RJ: Neuronal GLP1R mediates liraglutide's anorectic but not glucose-lowering effect. J Clin Invest 2014;124:2456-2463
29. Kanoski SE, Rupprecht LE, Fortin SM, De Jonghe BC, Hayes MR: The role of nausea in food intake and body weight suppression by peripheral GLP-1 receptor agonists, exendin-4 and liraglutide. Neuropharmacology 2012;62:1916-1927
30. Adams JM, Pei H, Sandoval DA, Seeley RJ, Chang RB, Liberles SD, Olson DP: Liraglutide Modulates Appetite and Body Weight Via GLP-1R-Expressing Glutamatergic Neurons. Diabetes 2018;
31. Secher A, Jelsing J, Baquero AF, Hecksher-Sorensen J, Cowley MA, Dalboge LS, Hansen G, Grove KL, Pyke C, Raun K, Schaffer L, Tang-Christensen M, Verma S, Witgen BM, Vrang N, Bjerre Knudsen L: The arcuate nucleus mediates GLP-1 receptor agonist liraglutide-dependent weight loss. J Clin Invest 2014;124:4473-4488
32. Henry FE, Sugino K, Tozer A, Branco T, Sternson SM: Cell type-specific transcriptomics of hypothalamic energy-sensing neuron responses to weight-loss. Elife 2015;4
33. Mazella J, Beraud-Dufour S, Devader C, Massa F, Coppola T: Neurotensin and its receptors in the control of glucose homeostasis. Front Endocrinol (Lausanne) 2012;3:143
34. Auguet T, Aragones G, Berlanga A, Martinez S, Sabench F, Aguilar C, Villar B, Sirvent JJ, Del Castillo D, Richart C: Low Circulating Levels of Neurotensin in Women with Nonalcoholic Fatty Liver Disease Associated with Severe Obesity. Obesity (Silver Spring) 2017;
35. Barchetta I, Cimini FA, Leonetti F, Capoccia D, Di Cristofano C, Silecchia G, Orho-Melander M, Melander O, Cavallo MG: Increased plasma proneurotensin levels identify NAFLD in adults with and without type 2 diabetes. J Clin Endocrinol Metab 2018;
36. Mendez M, Souaze F, Nagano M, Kelly PA, Rostene W, Forgez P: High affinity neurotensin receptor mRNA distribution in rat brain and peripheral tissues. Analysis by quantitative RT-PCR. J Mol Neurosci 1997;9:93-102
37. Piatek J, Mackowiak P, Krauss H, Nowak D, Bogdanski P: In vivo investigations of neurotensin receptors in adipocytes, hepatocytes and enterocytes of rat. Ann Agric Environ Med 2011;18:433-436
38. Schroeder LE, Leinninger GM: Role of central neurotensin in regulating feeding: Implications for the development and treatment of body weight disorders. Biochim Biophys Acta Mol Basis Dis 2018;1864:900-916
39. Beiroa D, Imbernon M, Gallego R, Senra A, Herranz D, Villarroya F, Serrano M, Ferno J, Salvador J, Escalada J, Dieguez C, Lopez M, Fruhbeck G, Nogueiras R: GLP-1 agonism stimulates brown adipose tissue thermogenesis and browning through hypothalamic AMPK. Diabetes 2014;63:3346-3358

40. Nonogaki K, Kaji T: The acute anorexic effect of liraglutide, a GLP-1 receptor agonist, does not require functional leptin receptor, serotonin, and hypothalamic POMC and CART activities in mice. Diabetes Res Clin Pract 2016;120:186-189
41. Burmeister MA, Ayala JE, Smouse H, Landivar-Rocha A, Brown JD, Drucker DJ, Stoffers DA, Sandoval DA, Seeley RJ, Ayala JE: The Hypothalamic Glucagon-Like Peptide 1 Receptor Is Sufficient but Not Necessary for the Regulation of Energy Balance and Glucose Homeostasis in Mice. Diabetes 2017;66:372-384
42. Kanoski SE, Hayes MR, Skibicka KP: GLP-1 and weight loss: unraveling the diverse neural circuitry. Am J Physiol Regul Integr Comp Physiol 2016;310:R885-895
43. Hauge M, Vestmar MA, Husted AS, Ekberg JP, Wright MJ, Di Salvo J, Weinglass AB, Engelstoft MS, Madsen AN, Luckmann M, Miller MW, Trujillo ME, Frimurer TM, Holst B, Howard AD, Schwartz TW: GPR40 (FFAR1) - Combined Gs and Gq signaling in vitro is associated with robust incretin secretagogue action ex vivo and in vivo. Mol Metab 2015;4:3-14

Table 1 Blood biochemistry

	Vehicle	Liraglutide	P-NT	P-NT + Liraglutide
Triglycerides (mg/dL)	95.1±15.2	82.2±9.0	100.4±17.4	82.2±15.7
Leptin (pg/mL)	48.1±9.9	42.3±11.8	35.4±12.7	21.7±3.5*
Insulin (ng/mL)	6.4±3.0	5.3±2.2	4.9±2.4	2.3±1.9*
Glucose (mM)	8.3±0.9	6.7±0.9**	8.4±0.8	6.4±0.4**

Values denote mean ± SD. *p<0.05 difference against vehicle. **p<0.01 difference against vehicle and P-NT. Data tested with one-way ANOVA with Tukey's multiple comparison test. n=6.

Figure legends

Figure 1 Metabolic effects of P-NT, liraglutide and P-NT+liraglutide combination-therapy in obese mice during 6-days treatment. A) Body weight, B) Cumulative food intake, C) Fat mass and D) Lean mass following treatment with vehicle, P-NT (396 nmol/kg), liraglutide (8 nmol/kg) or combination treatment with P-NT (396 nmol/kg) and liraglutide (8 nmol/kg). *p<0.05, **/##p<0.01, ###p<0.001 ****p<0.0001. **** in A and B denotes difference between combination-treatment and all other conditions. Data tested with two-way ANOVA repeated measurements with Tukey's multiple comparison test for individual time points (A, B) and one-way ANOVA with Sidak's multiple comparison test (C, D). Data are mean ± SD. n=6.

Figure 2 Indirect calorimetry, taste aversion, pharmaco-kinetics and taste preference. A) Energy expenditure, B) Weight adjusted energy expenditure, C) Activity levels, D) RER, E) Body weight, F) Food intake, G) Body weight with pair-feeding, H) Saccharin preference ratio during taste aversion, I) Intact neurotensin levels following peptide injections, J) Taste preference with simultaneous 2-diet access, K-L) Food intake inhibition on a chow versus a palatable medium-fat high-sucrose diet (condensed milk diet). *p<0.05, **/##p<0.01, ***/###p<0.001. ****/####p<0.0001. **** in E denotes difference between combination-treatment and vehicle, while ##/#### denote differences between P-NT and liraglutide mono-treatment and combination treatment. Data tested with ANCOVA (A, B) one-way ANOVA with Sidak's multiple comparison test (C, D, F and H) two-way ANOVA repeated measurements with Tukey's multiple comparison test for individual time points (E) and two-way ANOVA with Tukey's multiple comparison test (J-L). Data

are mean ± SD. n=8 (A-F, H and J-L), n=5 (G) and n=4 (I). Liraglutide dosed in a concentration of 2 nmol/kg (A-F and J-L) and 3 nmol/kg (G-I).

Figure 3 Multiplex fluorescence *in situ* hybridization (M-FISH) staining of GLP-1R, NtsR1and Pomc mRNA in the murine arcuate nucleus. A) Representative merged confocal image of arcuate nucleus section co-stained with probes (Pr) specific for GLP-1R (green), NtsR1 (magenta) and Pomc (orange) mRNA transcripts using M-FISH and counterstained with DAPI (blue). Insets show cells in higher magnification in B. Scale bar = 100 μm. B) Selected areas from above showing neurons co-stained with Pomc- (orange, column 1), NtsR1- (magenta, column 2), GLP-1R-transcripts (green, column 3) and a merged picture (column 4). Dashed line outline cytosol border. Scale bar = 5 μm. ME: Median eminence; 3V: 3rd Ventricle.

Figure 4 Neurotensin and liraglutide effects on Pomc neuron activity. A) Brightfield illumination of Pomc-hrGFP neuron, B) The neuron under fluorescein isothiocyanate (FITC; hrGFP) illumination, C) Complete dialysis of Alexa Fluor 350 from the intracellular pipette, D) Merged image illustrates colocalization of brightfield, hrGFP, and Alexa Fluor 350 indicative of a Pomc neuron. Scale bar = 50 μm, E) Current-clamp recording demonstrates that NT (100 nM) depolarized Pomc neurons, F) current-clamp recording demonstrates a Pomc-hrGFP neuron is depolarized by NT (100 nM) and liraglutide (100 nM), G) NT, liraglutide and combination-treatment induced change in membrane potential. Data are mean ± SD. **p<0.01, ****p<0.0001. Data tested with one-way ANOVA with Tukey's multiple comparison test n=3-7.

Figure 5 Role of the melanocortin system for P-NT, liraglutide and combination-therapy effects. A) Body weight loss following liraglutide (2 nmol/kg) treatment, B) Body weight loss following P-NT (396 nmol/kg) treatment, C) Body weight loss following P-NT (396 nmol/kg) + liraglutide (2 nmol/kg) treatment, D) Cumulative food intake following liraglutide (2 nmol/kg) treatment, E), Cumulative food intake following P-NT (396 nmol/kg) treatment F) Cumulative food intake following P-NT (396 nmol/kg) + liraglutide (2 nmol/kg) treatment, G) Change in fat mass, H) Change in lean mass. Data represent differences between MC4R KO mice and weight-matched DIO controls during 3 days treatment. */#/§p<0.05, ##p<0.01, ***/###/§§§p<0.001, ****/####/§§§§p<0.0001. */***/**** represent differences between DIO treatment and MC4R KO treatment, #/##/###/#### represent differences between DIO vehicle and DIO treatment and §/§§§/§§§§ represent differences between MC4R KO vehicle and MC4R KO treatment. Data tested with two-way ANOVA repeated measurements with Tukey's multiple comparison test for individual time points (A-F) and two-way ANOVA with Sidak's multiple comparison test (G-H). Data are mean ± SD. n=6.

Figure 6 Glucose tolerance after acute treatment with P-NT, liraglutide and P-NT+liraglutide combination-therapy in DIO mice. A) Glucose levels at individual time points, B) Glucose area under the curve, C) Insulin levels at individual time points following vehicle, P-NT (396 nmol/kg), liraglutide (2 nmol/kg) or combination treatment with P-NT (396 nmol/kg) and liraglutide (2 nmol/kg). * denotes differences between P-NT and liraglutide and P-NT and vehicle. Data tested with two-way

ANOVA repeated measurements with Tukey's multiple comparison test (A), one-way ANOVA with Tukey's multiple comparison test (B) and two-way ANOVA with Tukey's multiple comparison test (C). Data are mean ± SD. n=14.

Figure 7 Effects of 6 days treatment with P-NT, liraglutide or combination therapy on liver function and plasma cholesterol. A) Hematoxylin & Eosin stain (scale bar 500 = μm / zoom = 100 μm), B) Steatohepatitis score C) Hepatic gene expression related to cholesterol/lipoprotein uptake and D) Hepatic gene expression related to cholesterol and bile acid metabolism/ efflux, E) Total cholesterol and F) Lipoprotein profile following vehicle, P-NT (396 nmol/kg), liraglutide (8 nmol/kg), and P-NT (396 nmol/kg) + liraglutide (8 nmol/kg) treatment. *p<0.05, **p<0.01, ****p<0.0001. Data tested with Student's t-test (C-D) and one-way ANOVA with Tukey's multiple comparison test (E). Data are mean ± SD. n=6.

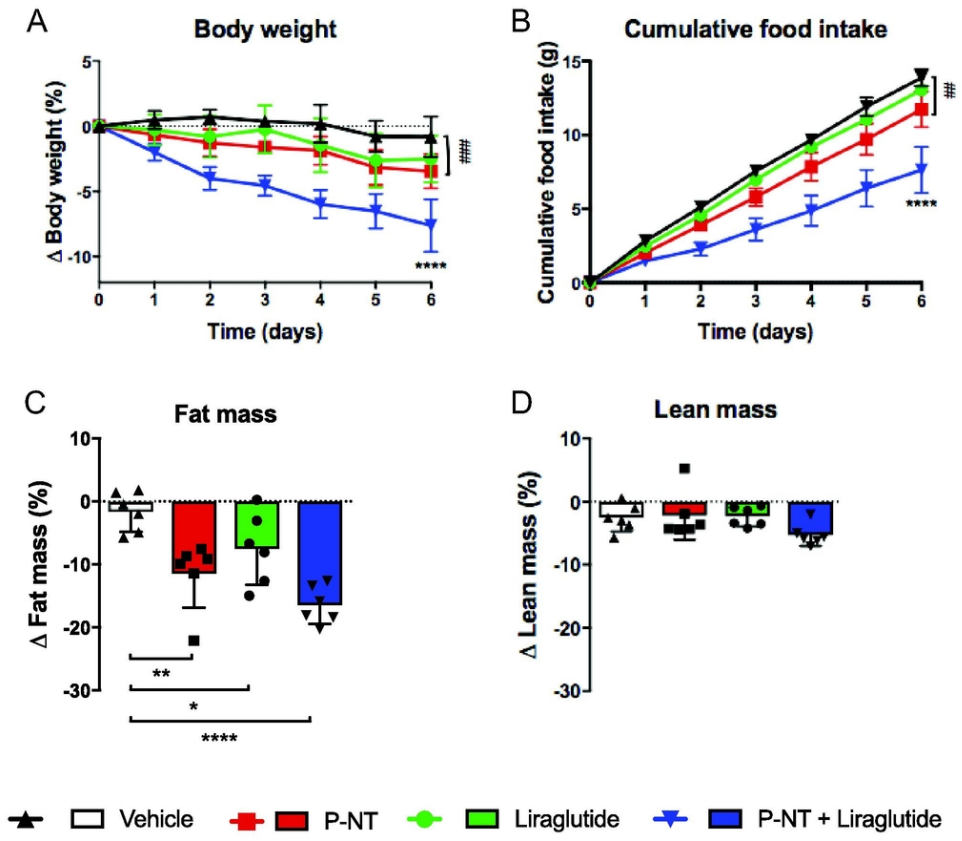

Figure 1 Metabolic effects of P-NT, liraglutide and P-NT+liraglutide combination-therapy in obese mice during 1 week treatment

88x74mm (300 x 300 DPI)

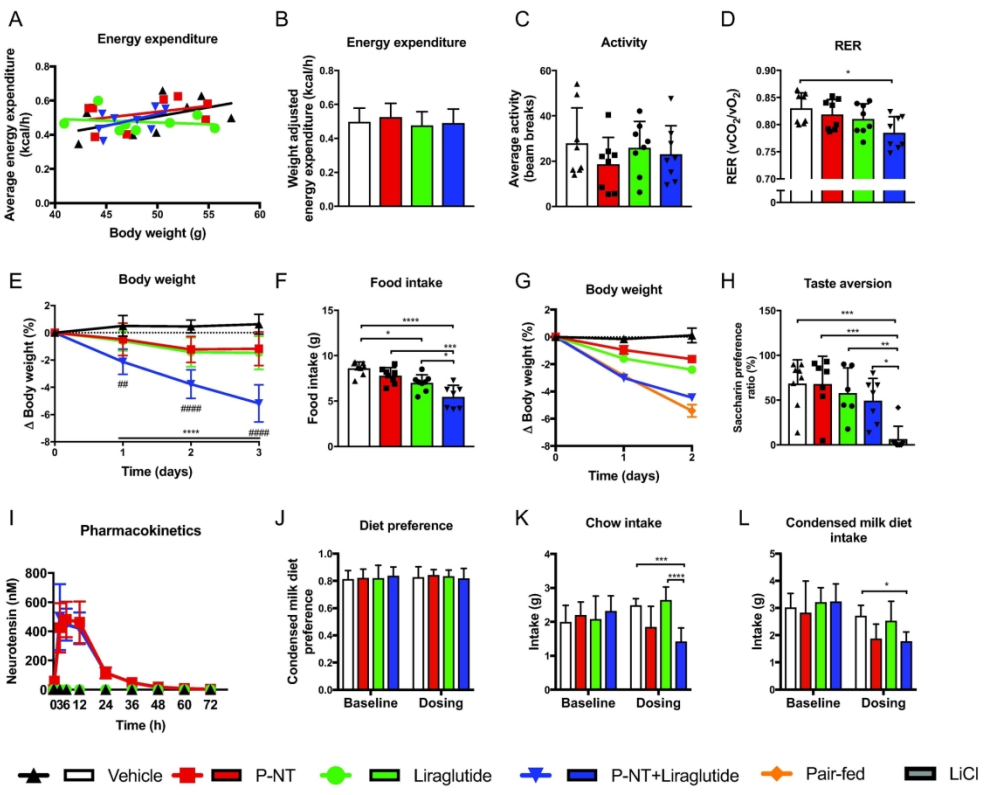

Figure 2 Indirect calorimetry, taste aversion, pharmaco-kinetics and taste preference

177x141mm (300 x 300 DPI)

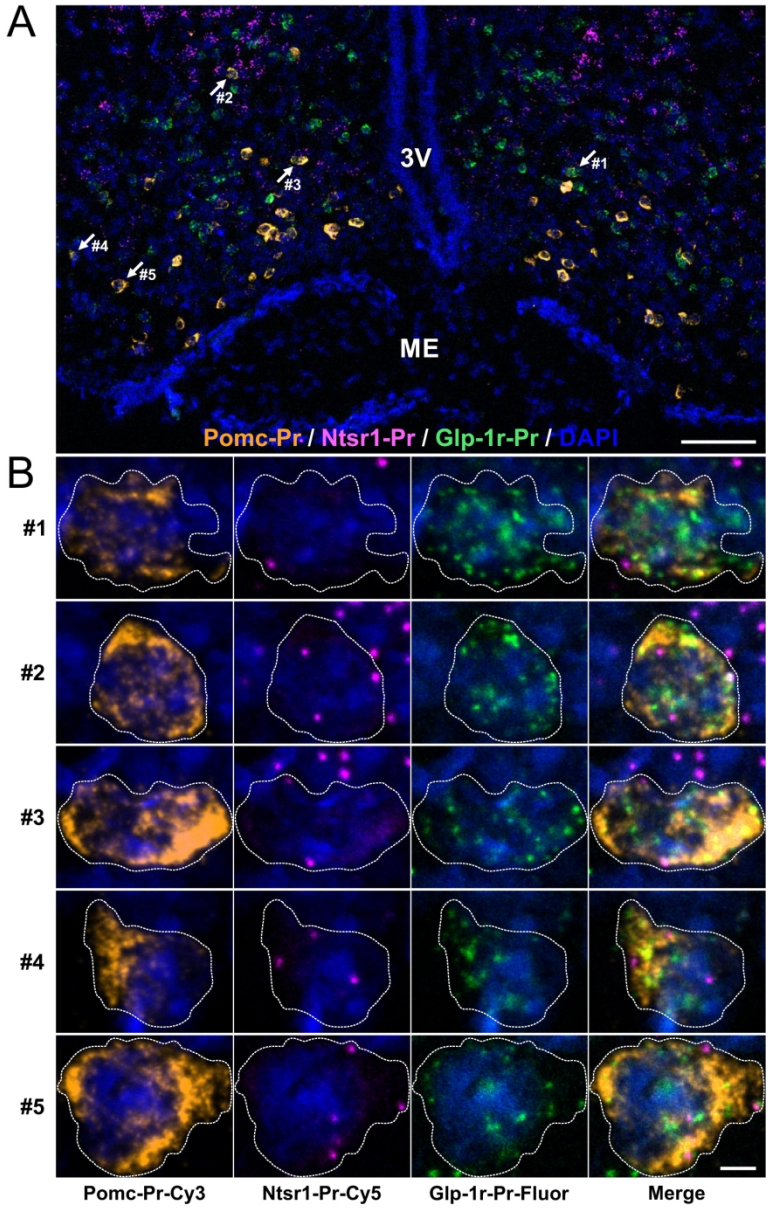

Figure 3 Multiplex fluorescence in situ hybridization (M-FISH) staining of GLP-1R, NtsR1and Pomc mRNA in the murine arcuate nucleus

180x284mm (300 x 300 DPI)

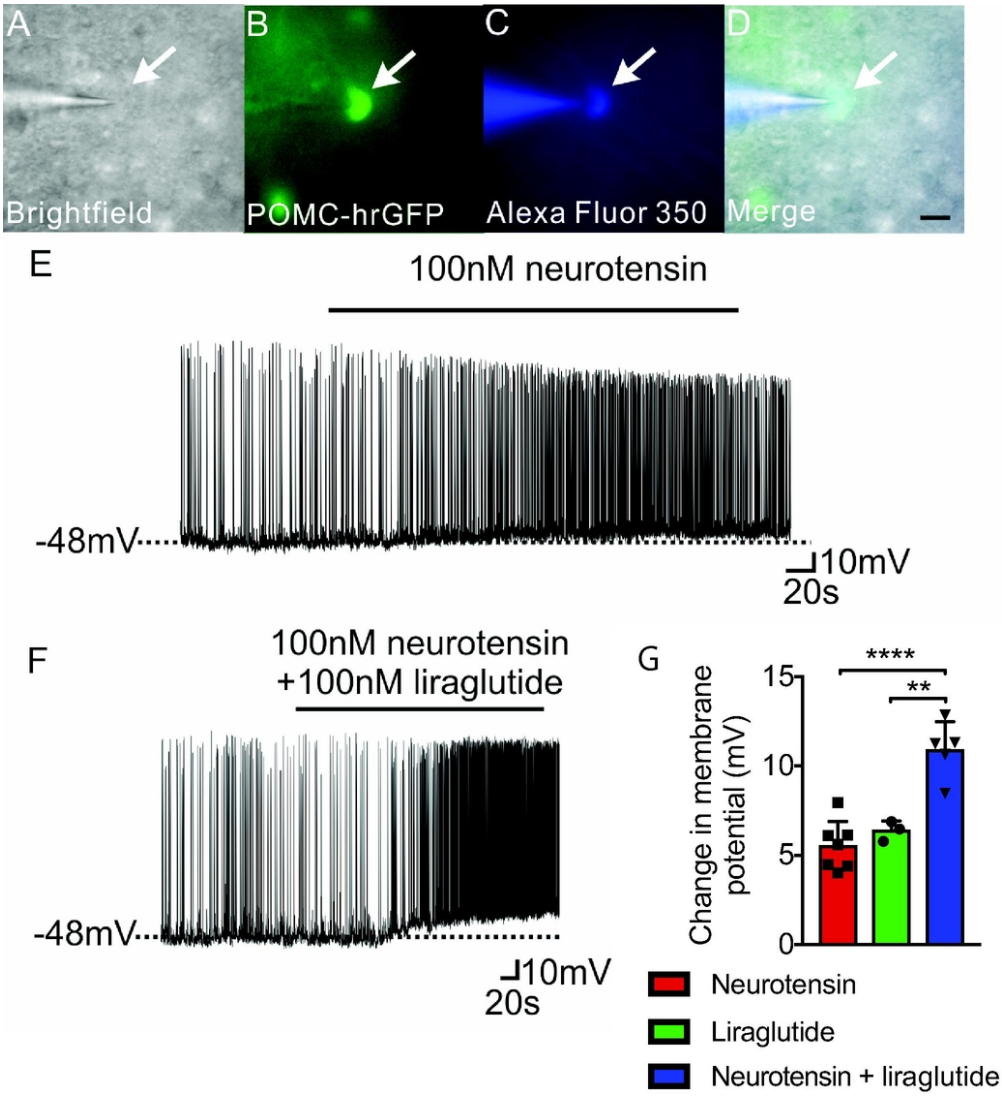

Figure 4 Neurotensin and liraglutide effects on Pomc neuron activity

87x95mm (300 x 300 DPI)

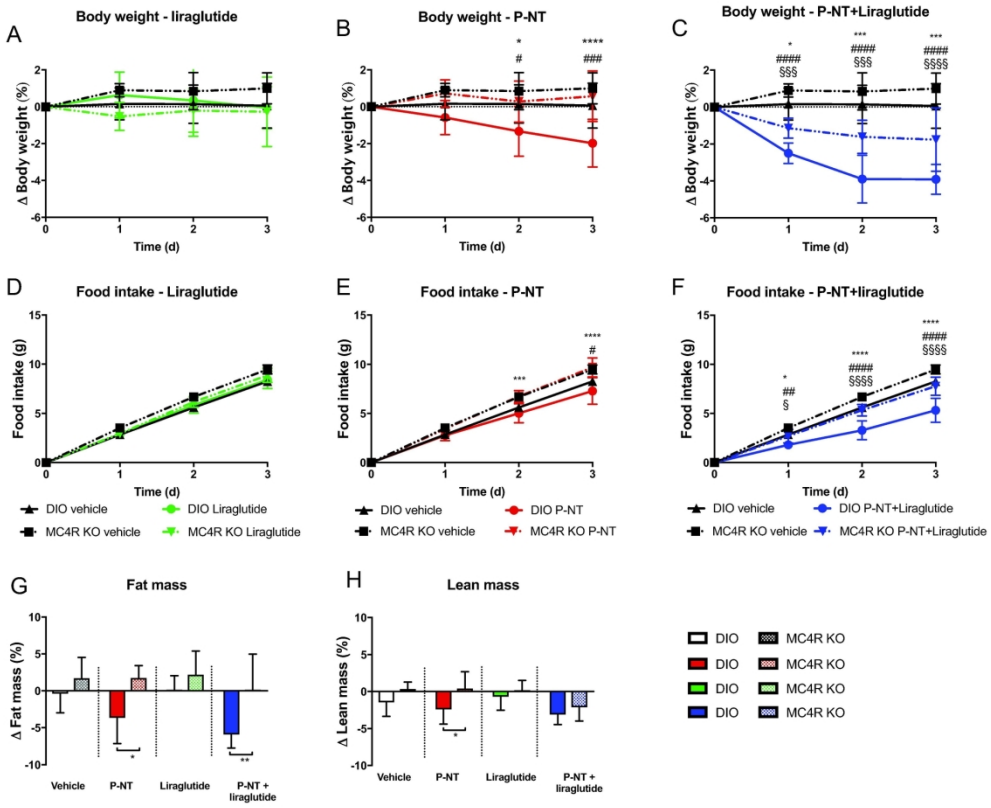

Figure 5 Role of the melanocortin system for P-NT, liraglutide and combination-therapy effects

180x153mm (300 x 300 DPI)

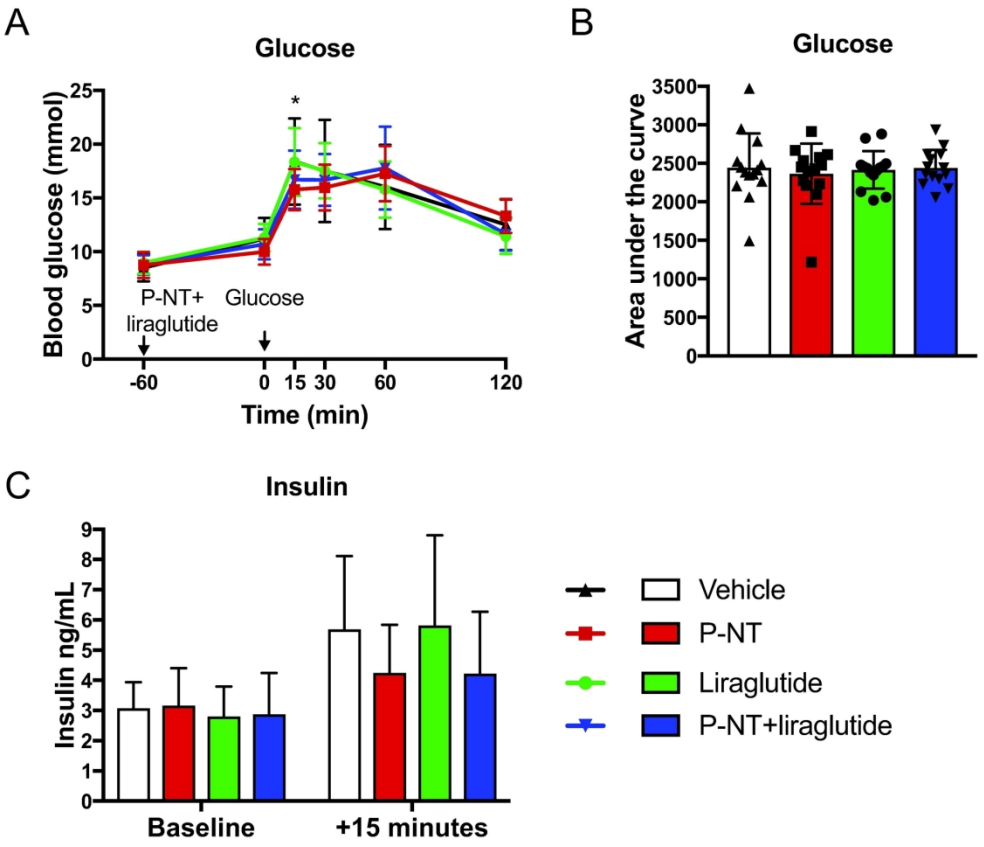

Glucose tolerance after acute treatment with P-NT, liraglutide and P-NT+liraglutide combination-therapy in DIO mice

175x151mm (300 x 300 DPI)

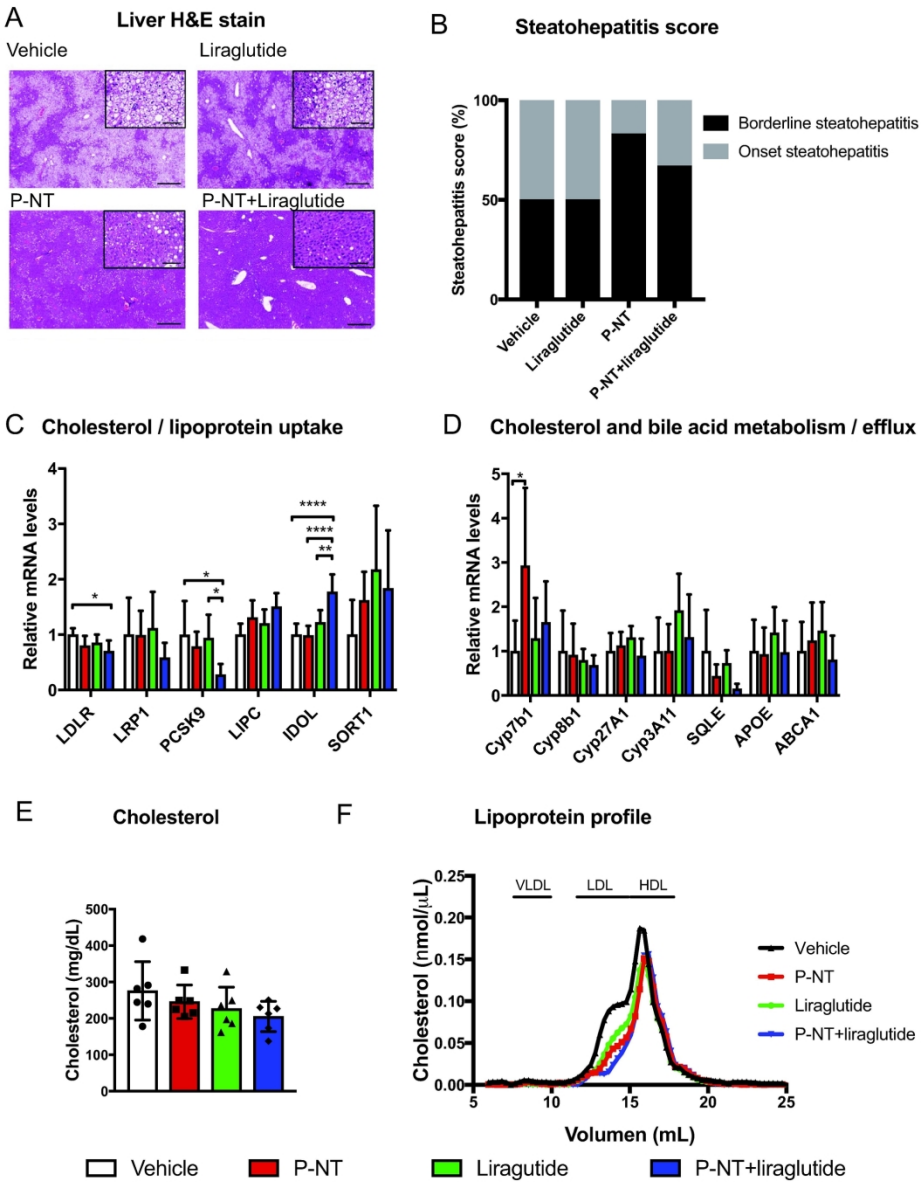

Effects of 6 days treatment with P-NT, liraglutide or combination therapy on liver function and plasma cholesterol

180x233mm (300 x 300 DPI)

Figure S1 Dose optimization of the P-NT dose A) Body weight and B) Food intake during 6 days of treatment for vehicle, liraglutide (8 nmol/kg), P-NT (396 nmol/kg), P-NT (1188 nmol/kg), P-NT (396 nmol/kg) + liraglutide (8 nmol/kg) and P-NT (1188 nmol/kg) + liraglutide (8 nmol/kg), C) Body weight and D) Food intake during 3 days of treatment for vehicle, Liraglutide (2 nmol/kg), P-NT (44 nmol/kg), P-NT (132 nmol/kg), P-NT (396 nmol/kg), P-NT (44 nmol/kg) + liraglutide (2 nmol/kg), P-NT (132 nmol/kg) + liraglutide (2 nmol/kg) and P-NT (396 nmol/kg) + liraglutide (2 nmol/kg). Data are mean ± SD. n=6.

Figure S2 Multiplex fluorescence *in situ* hybridization (M-FISH) control studies in the murine arcuate nucleus.

A) Representative confocal images of the arcuate nucleus section stained with probes specific for the housekeeping gene (positive control) *Mus musculus* Peptidylpropyl isomerase B (Ppib) mRNA with either fluorescein (Fluor), Cyanine3 (Cy3) or Cyanine5 (Cy5) demonstrating no or negligible crosstalk between the respective channels. B) Same as above, however stained with probes specific for *Bacillus subtilis* dihydrodipicolinate reductase (DapB) mRNA as a negative control demonstrating no staining in any channels. Nuclei was visualized with DAPI counterstaining (blue). Scale bars, 20 μm. n=3 mice.

Figure S3 Depolarization of Pomc neurons by neurotensin and liraglutide in the presence of tetrodotoxin. A) Representative electrophysiological trace demonstrating that the NT induced depolarization of Pomc-hrGFP neurons persists in the presence of TTX, B) Representative electrophysiological trace demonstrating that

the NT and liraglutide induced depolarization of Pomc-hrGFP neurons persists in the presence of TTX, C) NT and NT+liraglutide induced changes of membrane potential of POMC neurons with pretreatment of TTX. Error bars indicate SD. Data tested with Mann-Whitney non-parametric test n=4-5.

Figure S4 Effect of high dose liraglutide mono-therapy in MC4R KO mice compared to DIO controls. A) Body weight, B) Cumulative food intake. #p<0.05, ##p<0.01, ###p<0.001, ****/####/§§§§p<0.0001. **** represent differences between DIO vehicle and DIO liraglutide, #/##/###/#### represent differences between DIO liraglutide and MC4R KO liraglutide, §§§§ represent differences between MC4R KO vehicle and MC4R KO liraglutide. Data tested with two-way ANOVA repeated measurements with Tukey's multiple comparison test for individual time points. Data are mean ± SD. n=6.

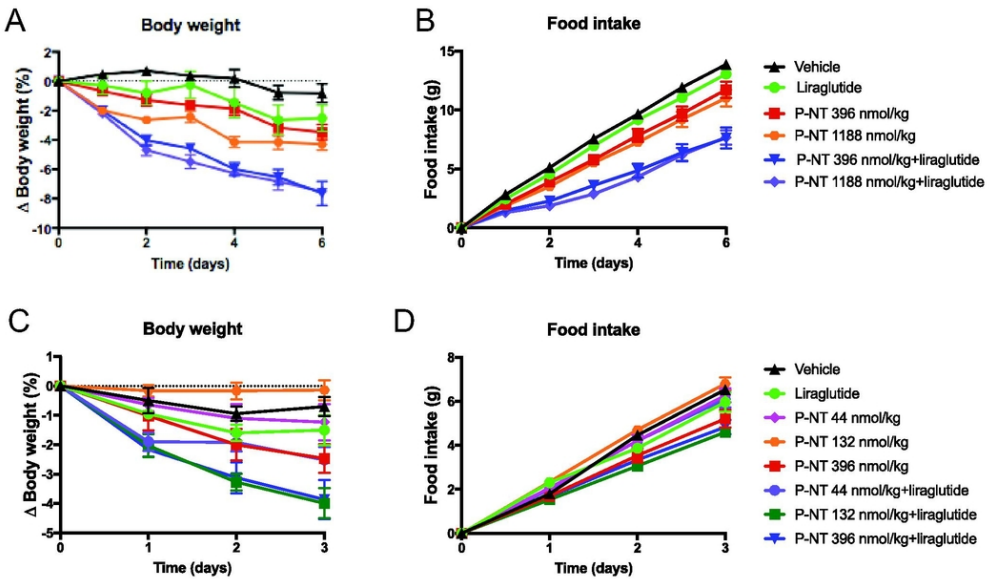

88x52mm (300 x 300 DPI)

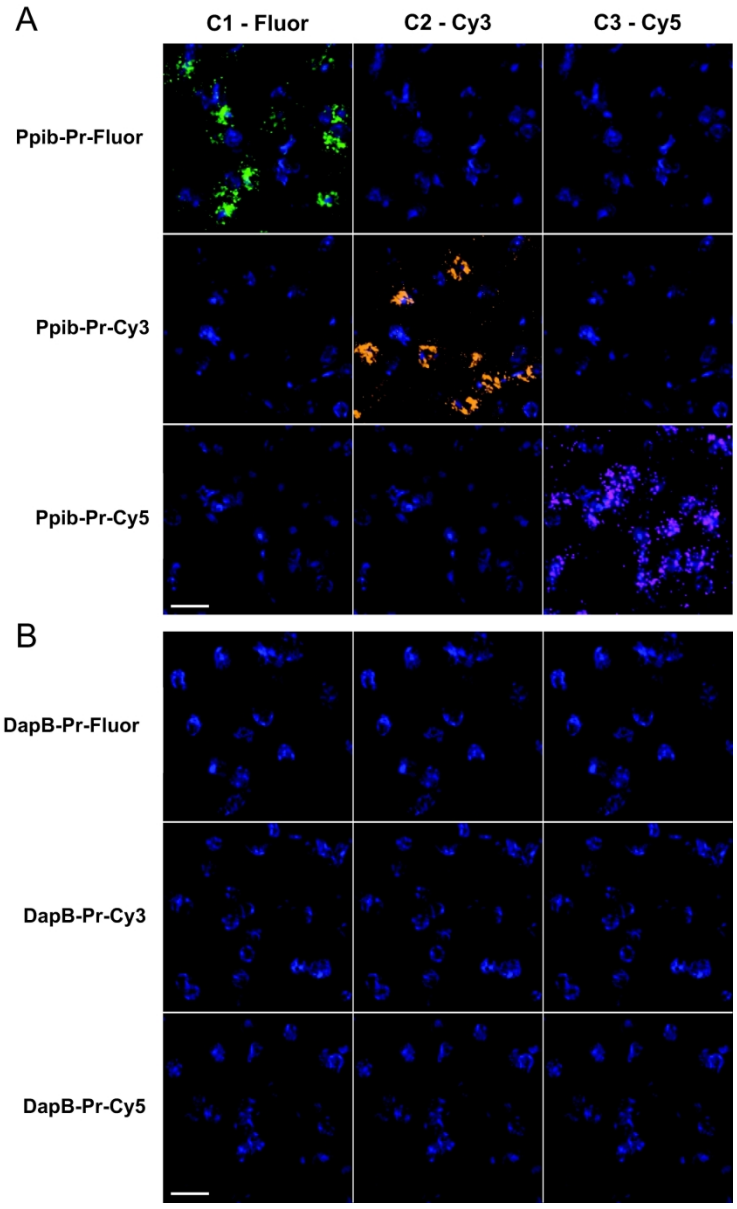

185x305mm (300 x 300 DPI)

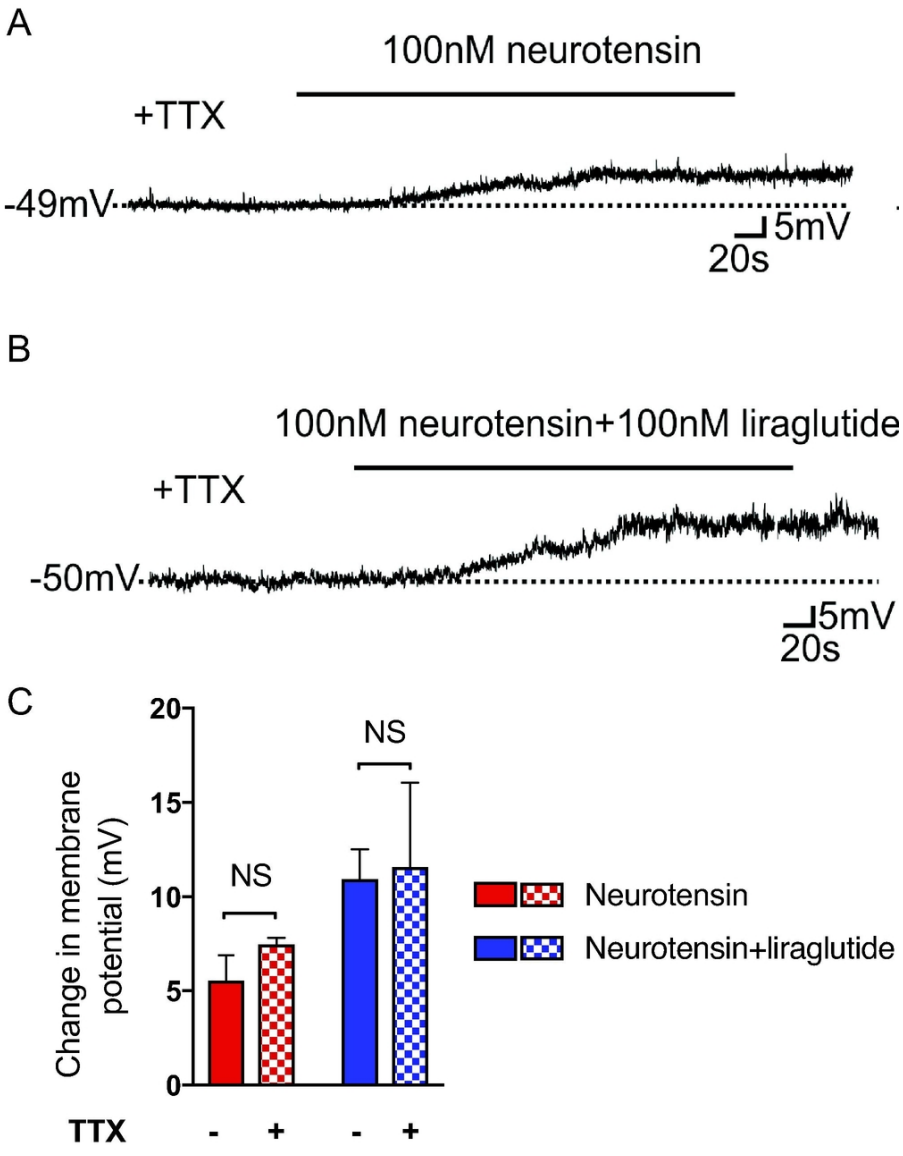

86x113mm (300 x 300 DPI)

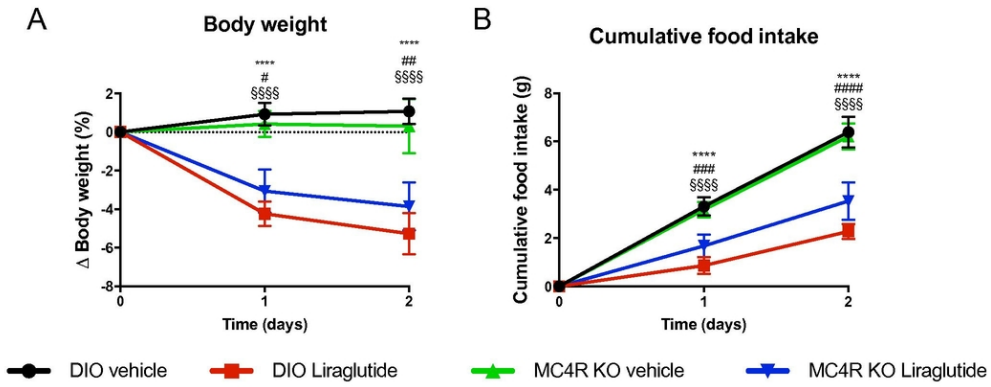

88x38mm (300 x 300 DPI)

Supplemental Table 1 Primers

Gene	Forward primer	Reverse primer
HPRT	CTTTGCTGACCTGCTGGATT	TTTCCAGTTAAAGTTGAGAGATCA
TBP	TCAAACCCAGAATTGTTCTCC	GGTAGATGTTTTCAAATGCTTCA
LDLR	TCAGACGAACAAGGCTGTCC	CCATCTAGGCAATCTCGGTCTC
LRP1	AACCTTATGAATCCACGCGC	TTCTTGGGGCCATCATCAGT
PCSK9	CACCCTGGATGCTGGTATCT	GACCTCTTCCCTGGCTTCTT
LIPC	ATGTGGGGTTAGTGGACTGG	TTGTTCTTCCCGTCCATGGA
IDOL	AGGACTGTCTCAACCAGGTG	TGCCTTGTCTGCTCCTGTAA
SORT1	ATCCCAGGAGACAAATGCCA	AACCTTCCGCCACAGACATA
Cyp7b1	TCTGGGCCTCTCTAGCAAAC	GCACTTCTCGGATGATGCTG
Cyp8b1	CAGCGGACAAGAGTACCAGA	TGGATCTTCTTGCCCGACTT
Cyp27A11	CTTCATCGCACAAGGAGAGC	CCAAGGCAAGGTGGTAGAGA
Cyp3A11	CTCTCACTGGAAACCTGGGT	TCTGTGACAGCAAGGAGAGG
SQLE	TGTTGCGGATGGACTCTTCT	GAGAACTGGACTGGGGTTGA
APOE	GATCAGCTCGAGTGGCAAAG	TAGTGTCCTCCATCAGTGCC
ABCA1	AAAACCGCAGACATCCTTCAG	CATACCGAAACTCGTTCACCC